

Whitecap Phenomenology for Ocean Surface Simulation

Jerry Tessendorf, Colin Reinhard, Liang Gao

March 2, 2023



Figure 1: Rendered maritime scene, including the whitecap opacity map, with whitecap fraction $W = 0.15$, windspeed is 20.4 m/s, and rms waveheight is 2.6 m.

Abstract

In many computer graphics applications involving rendering of maritime scenes, ocean whitecaps are generated via a minimum eigenvalue threshold and decay process. The few parameters involved are typically set by a user for visual impact, without regard to knowledge of oceanographic phenomenology. Here a process is described for the threshold parameters by (a) establishing an ensemble-averaged relationship between the threshold and the whitecap fraction, (b) selecting a phenomenological model for whitecap fraction in terms of wind speed and possibly other parameters, and (c) using simulation data to estimate the Probability Density Function for the ocean surface minimum eigenvalue ensemble to create a Cumulative Distribution Function (CDF) for the threshold value.

1 Introduction

The simulation of an ocean surface as a height field is a part of many applications in graphics, maritime operations, games, and films. The height field representation is compact and efficient to compute, and is anchored in oceanographic phenomenology. Complex random surfaces derive from statistical models of the spatial and temporal spectra of waves under a variety of geographic and oceanographic conditions. As an effectively 2D data set, height fields can be manipulated toward stylized surface designs and artistic user goals.

While the height field representation captures spatial and temporal motions that are physically realistic, it cannot capture many fluid phenomena that occur on and near the surface. For example, wave breaking has not been represented as a height field, although detailed nonlinear simulations have demonstrated height fields becoming very sharp leading up to the transition to breaking [9, 11] before becoming numerically unstable. The “cuspy displacement” algorithm [13] allows horizontal displacements of the height field while remaining stable, can lead to arbitrarily sharp peaks on the waves, and can even cause nonphysical passage of the surface around the wave peak through itself when and where it is natural for the wave surface to break. Fully three dimensional water simulation systems can achieve a much more accurate representation of wave breaking [6].

Turbulence and spray during wave breaking produce long-lasting patches of foam and bubbles on and just below the surface. Generically referred to as whitecaps, the detailed phenomena of its optical properties, emission and temporal persistence involve air-sea interface physics, and chemical and biological content of the water. Whitecaps have two key properties that make it useful to characterize them phenomenologically: (1) they persist for long periods of time, from seconds to minutes depending on environmental conditions; (2) the fine detail bubbles and structure inside whitecaps, and the spatial size of individual whitecap spots, give them high contrast with adjacent water regions across a broad spectrum of wavelengths, from ultraviolet through infrared bands, and even in microwave bands. The combination of these two properties have allowed a number of observations – using instruments at sea, airborne, and overhead – to characterize whitecaps with phenomenological models of their spatial distribution. Many such studies relate the fraction of surface area occupied by whitecaps (Whitecap Fraction, or W), to the wind speed above the ocean surface (U). A collection of these phenomenological relationships are summarized in [15, 10], and they typically have the form

$$W = a (U - U_0)^b \tag{1}$$

where a , b , and U_0 are model parameters that are fit to observational data. Of course W is dependent on many more factors than just the wind speed U , which is reflected in variance of model parameter values across the analyses of the various data sets in [3], for example. Equation 1 acts as an organizational tool for further studying the fuller, complex relationship. Models expressing W in terms of ocean spectral model parameters in [15, 8] are recent attempts to explore more deeply. In this paper, we adopt the outlook that any of these models could be of interest, and a practitioner of ocean surface simulation should have the option to select any specific one that best matches the goals of their simulation efforts.

Whitecaps generated in the context of height field ocean surface simulations are stored as 2D textures that represent the opacity of the whitecaps in a given location. Several methods to initiate whitecap formation at a location on the ocean surface are (1) compute the vertical acceleration and increase the value of the whitecap texture map when the vertical acceleration exceeds a user-decided

fraction of g (the constant of gravity), assuming that threshold exceedance happens on or near the wave peak[14] (note that [14] used a whitecap fraction model to set the value of the fraction of g); (2) compute the local curvature, and increase the value of the whitecap texture when the curvature magnitude exceeds a user-decide threshold value; (3) for “cuspy displaced” waves, use a user-selected threshold to test the minimum eigenvalue, λ_{min} , of the local 2D Jacobian of the cuspy displacement[13, 2]. In this paper we focus on this eigenvalue test. The two eigenvalues of the Jacobian are dimensionless. Where the displacement is zero, the minimum eigenvalue is 1, and where the cuspy displacement produces a sharp peak the minimum eigenvalue approaches zero. A negative-valued minimum eigenvalue corresponds to the unphysical case of the surface passing through itself, a case we exclude. The test checks for locations where λ_{min} drops below a threshold value λ_T . This mechanism does not connect in a direct way with the observed phenomenology for whitecap fraction W . In order to produce whitecaps consistent with the known phenomenology, the choice of threshold should be related to the ocean surface parameterization, the whitecap texturemap generation model, and the phenomenology of whitecap fraction.

A specific approach for selecting the threshold is described in algorithm 1. The reasoning for this algorithm is presented in section 3. The realized whitecap map produced from an ocean surface simulation and this algorithm will have a whitecap fraction that is close to the value of W from the phenomenological model, but not guaranteed to be equal to W . There are many parameters – such as the water salinity, particulate matter and dissolved organic matter concentrations, and water depth – that determine the actual whitecap fraction in a specific ocean surface realization, in addition to wind speed and minimum eigenvalue threshold. The other remaining parameters also have an impact, as does the set of random numbers used to create the random realization. But many realizations generated with this algorithm will have whitecap fractions clustered around the model prediction. This is shown in section 5.

This paper describes the novel set of steps for data generation, data analysis, and model creation to assign a value to the threshold in terms of the whitecap fraction and the cumulative distribution function of the random field of minimum eigenvalues, following algorithm 1. The steps are illustrated with a simulation data set that produces specific results, but the intent is to describe and illustrate the overall method so that it could be applied in cases with different phenomenology models.

The next section considers previous work in creating computer graphic whitecap textures for particular game and feature film situations. Section 3 discusses a model for whitecap texture generation from the minimum eigenvalue threshold test and half-life decay, based on the methods described in section 2. This model also provides a method for computing whitecap fraction in any simulation frame. Procedures for extracting a λ_T using the probability density function and cumulative distribution function of λ_{min} produced by a realization, and the chosen whitecap fraction model are presented in section 4. Section 5 show that the whitecap fraction realizations are reasonably close to the chosen phe-

nomenological whitecap fraction model, and give visual demonstrations of the whitecap textures. Finally we summarize the paper and mention some additional potential approaches in section 6.

2 Previous Work

Simulation of an ocean surface as a height field with dispersive time evolution has been in use for a variety of computer graphic applications for some time[4, 7, 13]. The height at any horizontal location \mathbf{x} and time t is represented in terms of a Fourier amplitude \tilde{h} :

$$h(\mathbf{x}, t) = \int \frac{d^2k}{2\pi} \tilde{h}(\mathbf{k}, t) e^{i\mathbf{k}\cdot\mathbf{x}} \quad (2)$$

where \mathbf{k} is the two-dimensional wave vector Fourier integration variable, and \tilde{h} is decomposed at

$$\tilde{h}(\mathbf{k}, t) = \tilde{h}_0(\mathbf{k}) e^{i\omega(k) t} + \tilde{h}_0^*(-\mathbf{k}) e^{-i\omega(k) t} \quad (3)$$

using the dispersion relationship $\omega(k)$ for frequency in terms of the magnitude of the wave vector $k \equiv |\mathbf{k}|$. The complex amplitude \tilde{h}_0 is a random realization of amplitudes drawn from an ensemble that is driven by the directional wave power spectral density $P(\mathbf{k})$ provided by oceanographic phenomenology. This scheme is typically implemented on a rectangular horizontal spatial grid of points \mathbf{x} , a complementary grid of wave vectors \mathbf{k} , and the Fast Fourier Transform (FFT) operation to perform the transform for any user-specified time t .

A Gerstner-like horizontal displacement at each horizontal point derives from the wave height expression via a Fourier Transform

$$\mathbf{D}(\mathbf{x}, t) = i \int \frac{d^2k}{2\pi} \frac{\mathbf{k}}{k} \tilde{h}(\mathbf{k}, t) e^{i\mathbf{k}\cdot\mathbf{x}} \quad (4)$$

and is also typically evaluated via FFT. This displacement moves the location of the wave height $h(\mathbf{x})$ to the horizontal location

$$\mathbf{x}_{cusp} = \mathbf{x} + f_{cusp} \mathbf{D}(\mathbf{x}, t) \quad (5)$$

where the cusp scale factor f_{cusp} is a user-decided value to select how much horizontal displacement to apply. This horizontal displacement is a change of variables that effectively alters the two-dimensional area of the surface, with the amount of change measured by the determinant of the Jacobian matrix of the change of variables

$$J(\mathbf{x}, t) = \mathbf{1}_{2D} + f_{cusp} \nabla \mathbf{D}(\mathbf{x}, t) \quad (6)$$

where $\mathbf{1}_{2D}$ is the 2D identity matrix. The determinant of J is decomposable as the product of its two eigenvalues, λ_{max} and λ_{min} , where $\lambda_{min} \leq \lambda_{max}$. Note that in the absence of displacements, e.g. for $f_{cusp} = 0$, both eigenvalues and

the determinant are 1. As the displacement becomes stronger, the determinant of J becomes smaller, the peaks of the waves become sharper and the troughs become rounded and broad. In the limit that the determinant of J is zero, the peak is singularly sharp. For $\det J < 0$, the wave peak passes through itself and is an undesirable artifact. The situation $\det J \leq 0$ is equivalent to the statement $\lambda_{min} \leq 0$, so it is reasonable to focus on the minimum eigenvalue as a marker of the amount of cuspliness caused by the displacement, and hence a marker for the onset of whitecaps. This also has the benefit of interpreting the minimum eigenvector as the horizontal direction in which the wave is “trying to break”.

Using the determinant of the Jacobian, [5] built a method of computing the presence of whitecaps for a lighting model. Their approach considers whether the determinant drops below a threshold value at any given location and produces an effective Lambertian reflectivity depending on how far beyond the threshold that the determinant has fallen, based a gaussian model for the probability distribution function of the determinant, and a cumulative distribution for the threshold value. This framework bears some similarity to the model in section 4, except that section 4 employs the minimum eigenvalue, rather than the determinant, as a more sensitive measure of peak sharpness, section 4 does not assume gaussian statistics, and section 4 applies the analysis to fix the threshold based on whitecap fraction, whereas [5] fix whitecap fraction based on threshold value. Physically, whitecaps persist at a given location for seconds to minutes after favorable conditions have passed for the Jacobian determinant to cross the threshold, which is not accounted for by [5]. The persistence over time is modeled by [12, 2] by tracking a whitecap value at any location using a texture map, with the value of the map decaying over time with a half life T . As waves pass over a location with decaying whitecap value, the value can be recharged if the wave minimum eigenvalue is favorable for the formation of whitecaps. This produces a spatially and temporally extended history of whitecaps. While rendering, this whitecap texture may not have sufficient spatial resolution for aesthetically desirable foam patterns and dynamics, and so the texture is sometimes used as a opacity with which to “pull through” a separately created (dynamic) artistically crafted detailed whitecap pattern. The opacity model discussed in detail in section 3 is essentially this one.

3 Whitecap Opacity and Fraction Model

The model used here for whitecaps is a basic description which could be extended in many ways and still be applicable in the section 4. The essential ingredient is that the whitecaps are represented by a spatial map $O(\mathbf{x}, t)$ that varies in value from 0 to 1, with 0 representing no whitecaps present, to 1 representing full whitecaps present. The simulation process is initialized by setting $O(\mathbf{x}, 0) = 0$ at all locations. The map is updated by two processes: (1) resetting the value to 1 at locations where whitecaps are being generated, and (2) decay the value of the map at locations where no generation is taking place. The update process

from time t to $t + \Delta t$ is:

$$O(\mathbf{x}, t + \Delta t) = \begin{cases} 1 & \lambda_{min}(\mathbf{x}, t + \Delta t) < \lambda_T \\ O(\mathbf{x}, t) e^{-\Delta t/T} & \lambda_{min}(\mathbf{x}, t + \Delta t) \geq \lambda_T \end{cases} \quad (7)$$

This can also be expressed as a simple update process using the Heaviside step function $\Theta(x)$ as

$$O(\mathbf{x}, t + \Delta t) = O(\mathbf{x}, t) e^{-\Delta t/T} + \Theta(\lambda_T - \lambda_{min}(\mathbf{x}, t + \Delta t)) \left(1 - O(\mathbf{x}, t) e^{-\Delta t/T}\right) \quad (8)$$

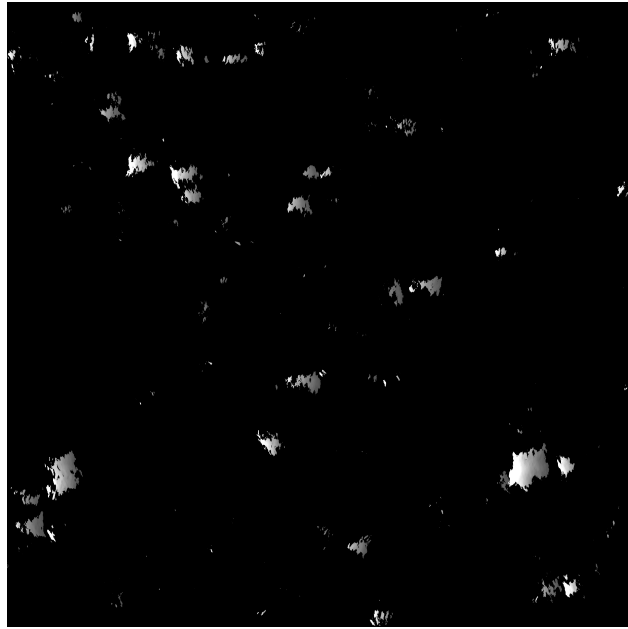
In this model, the amount of whitecaps produced at any location over an extended period of time is sensitive to the spatial spectrum $P(\mathbf{k})$, the random numbers in the realization, the magnitude of the horizontal displacement (which in turn follows from the magnitude of wave heights), the cusp scale parameter f_{cusp} , and the decay half life T . Figure 2 shows two examples of whitecap textures from this algorithm. All of the parameters except the threshold λ_T are the same between them, showing the very wide range of whitecap conditions that can be generated.

A value for whitecap fraction at time t follows directly from this construction of the whitecap texture. The value of O at any location can be interpreted as the amount of whitecaps at that location, and a value $W(t)$ for the whitecap fraction across the simulation grid is

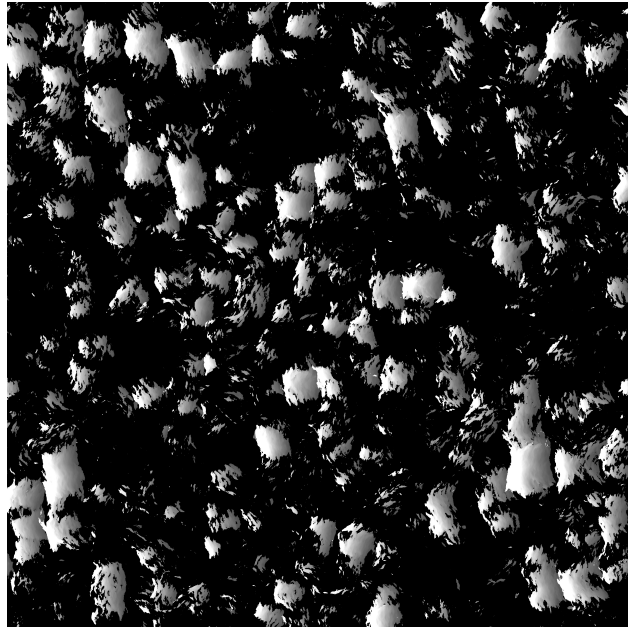
$$W(t) = \frac{1}{N_x N_y} \sum_{\mathbf{x}} O(\mathbf{x}, t) \quad (9)$$

which is summed over the $N_x \times N_y$ rectangular grid of points. This quantity is 1 when every grid point is full on, and zero when all grid points are empty. Figure 3 shows the whitecap fraction as a function of frame (time) for four different simulation conditions. The fraction grows for a period of time roughly equal to the half life T , undergoes some fluctuation for another half life, then roughly reaches a statistically steady state beyond two to three half lives.

Predicting the amount of whitecap fraction $W(t)$ from the set of simulation parameters is not practical or useful, because any value of W can be obtained in multiple ways from them. For example, even for a very calm ocean surface, which would not be predicted to have whitecaps based on physical experience, whitecaps can be produced by setting the threshold λ_T very close to 1. Alternatively, even for very large waves at high wind speed, the model can produce $W = 0$ simply by setting $f_{cusp} = 0$. An algorithm that produces physically reasonable whitecap fraction must allow for variations of all of these parameters in the recommended a value for λ_T , which can be made to agree with the empirically observed whitecap fraction models.



(a)



(b)

Figure 2: Whitecap textures at frame 1000 of a simulation, generated using equation 7. All parameters are the same for each, except the minimum eigenvalue threshold. (a) $\lambda_T = 0.71$, with $W = 0.011$. (b) $\lambda_T = 0.81$ and $W = 0.15$.

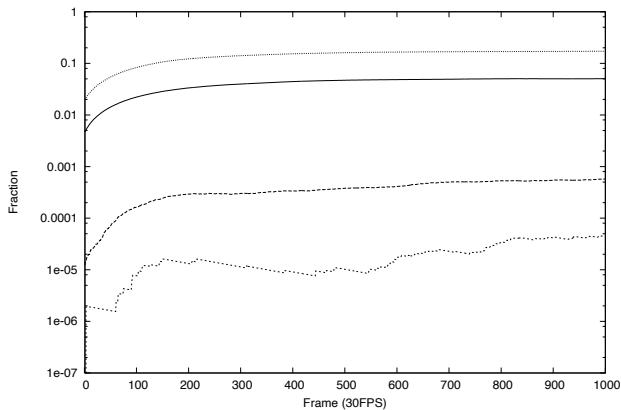


Figure 3: Whitecap fraction $W(t)$ computed for each frame, evolving from the start of the simulation to a statistically steady state, for several sets of simulation parameters. The 1000 frames represents 33.33 seconds of time. The half life is 8 seconds.

4 Threshold From Cumulative Statistics

To establish a procedure for obtaining λ_T for any particular ocean surface realization and phenomenological whitecap fraction model, the whitecap fraction update process can be used to estimate an ensemble averaged whitecap fraction, $\langle W \rangle$. It is this ensemble-averaged whitecap fraction that we identify with the whitecap fraction in phenomenological models like equation 1. The ensemble average is driven by random fluctuations in minimum eigenvalue, which in turn has its own ensemble of values drawn from a probability distribution. Further, we assume that both ensembles are statistically stationary and spatially homogeneous, so that $\langle W \rangle$ and the PDF of λ_{min} are time- and space-independent. Taking the ensemble average of equation 8, the connection between the whitecap fraction ensemble and the minimum eigenvalue ensemble is

$$\langle W \rangle = \langle W \rangle e^{-\Delta t/T} + \langle \Theta (\lambda_T - \lambda_{min}) \rangle - \langle W \Theta (\lambda_T - \lambda_{min}) \rangle e^{-\Delta t/T} \quad (10)$$

The coupled moment term $\langle W \Theta \rangle$ mixes the whitecap fluctuations – which fluctuate over a time scale of many seconds to minutes – with fluctuations of the minimum eigenvalue, which has a much shorter timescale for fluctuations. Because of the separation of these time scales, the moment is modeled as approximately separating into the product of the individual ensemble averages, $\langle W \Theta \rangle \approx \langle W \rangle \langle \Theta \rangle$. With this assumption, the ensemble averaged whitecap fraction is

$$\langle W \rangle = \frac{\langle \Theta \rangle}{1 - \alpha (1 - \langle \Theta \rangle)} \quad (11)$$

where $\alpha \equiv \exp(-\Delta t/T)$ is the temporal decay factor. During frame-by-frame simulation of the whitecap map, using the update in equation 7, the time step

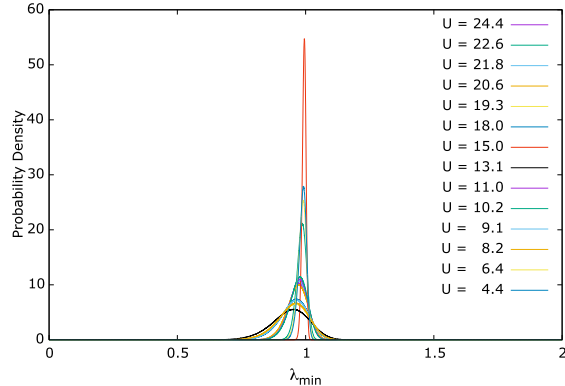


Figure 4: Probability Distribution Functions (PDFs) for the minimum eigenvalue for multiple ocean surface simulations with the indicated windspeeds U .

Δt is the time separation between frames. For ensemble averaging, this is not necessarily an appropriate value to use. The onset and growth of whitecaps can have a time scale of their own, shorter than the decay time, but independent of our simulation step time. In the ensemble averaged model, the parameter Δt , or equivalently α , is chosen from the analysis to achieve agreement with the whitecap phenomenology in equation 1.

Given a probability density function for the minimum eigenvalue, $P(\lambda_{min})$, the ensemble averaged Heaviside function is

$$\langle \Theta(\lambda_T - \lambda_{min}) \rangle = \int_0^{\lambda_T} d\lambda P(\lambda) \quad (12)$$

Here we exclude negative values of the minimum eigenvalue as unphysical. This is a Cumulative Distribution Function (CDF) for the PDF, and is a function of the threshold value λ_T . A very similar quantity appeared in [5], with two differences: (1) the full Jacobian was used there, whereas here we use the minimum eigenvalue, and (2) the PDF was assumed to be gaussian in [5], whereas here it is obtained from simulation data.

The process for obtaining the PDF and the CDF is based on sampling values of the minimum eigenvalue from frames of ocean surface simulation to assemble a histogram of λ_{min} . The PDF is the histogram after normalizing the histogram values so that the area under the histogram is 1. Figure 4 shows the PDF for several simulations of ocean surfaces. The simulations differ by making random selections of spectral model parameters for the TMA spectrum, and random choices for the physical size of the simulation patch. Each PDF is labelled according to its windspeed. Several properties of the PDFs are apparent from this figure.

1. The PDFs have significant non-gaussian tails, and so it is important to

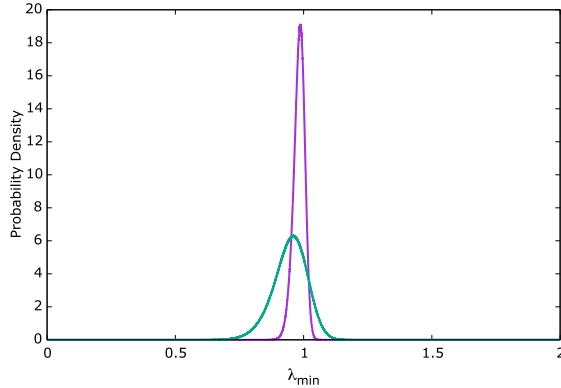


Figure 5: PDFs for two ocean surface simulations, both with windspeed $U = 11.1m/s$ but with other spectral parameters differing.

calculate the CDF directly rather than from an assumed PDF model form.

2. For a given windspeed, the width (and corresponding peak) can vary greatly. Figure 5 shows two PDF curves with similar windspeeds but with very different width and peak. Consequently, estimating the PDF directly from the simulation data is very important for capturing an accurate CDF.

From the data-driven PDF, a CDF is obtained by direct summation, as illustrated in figure 6.

This framework relating the whitecap fraction to the CDF can be restated as an implicit procedure for selecting of a threshold λ_T such that

$$\text{CDF}(\lambda_T) \equiv \langle \Theta \rangle = \frac{\langle W \rangle (1 - \alpha)}{1 - \alpha \langle W \rangle}. \quad (13)$$

Because the CDF is monotonic in λ_T , it is accurately inverted by a simple bounds test. This enables algorithm 1, which obtains a value for a threshold for any value of the whitecap fraction.

5 Results

Random realizations of ocean whitecap maps were generated using the TMA spectrum and spectrum parameters chosen at random in ranges displayed in table 1. The PDF of the minimum eigenvalue, and the CDF were generated from samples of a single frame of ocean surface. Generating the PDF from multiple frames of minimum eigenvalues produced little impact on the PDF. Following algorithm 1, the randomly chosen windspeed produced an average

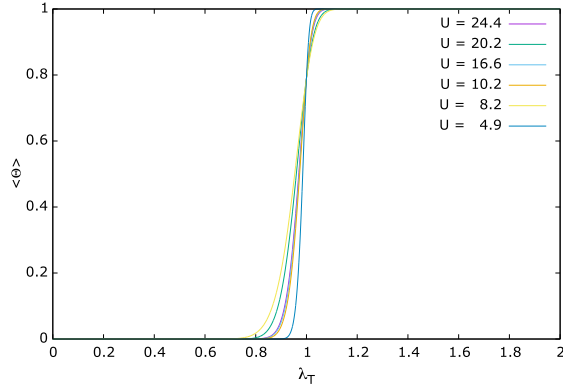


Figure 6: Cumulative Distribution Function (CDF) $\langle \Theta \rangle$ for several ocean surface simulations.

Algorithm 1 Algorithm for obtaining the minimum eigenvalue threshold for a particular ocean surface realization and a whitecap fraction model. The factor α is a model parameter equal to $e^{-0.15}$

1. User-selected Spectrum parameters, including wind speed U .
 2. Create random ocean surface realization
 3. Estimate Probability Density Function $P(\lambda_{min})$ from minimum eigenvalues of ocean surface realization.
 4. Create Cumulative Distribution Function $CDF(\lambda_T)$ for the threshold λ_T .
 5. $W \leftarrow a (U - U_0)^b$
 6. $W_{reduced} \leftarrow W (1 - \alpha) / (1 - \alpha W)$
 7. $\lambda_T \leftarrow CDF(\lambda_T) = W_{reduced}$
-

Parameter	Range
half life T (sec)	{ 4.0, 8.0 }
cuspscale f_{cusp}	{ 0.05, 0.95 }
wind speed U (m/s)	{ 4.0, 25.0 }
wind direction (deg)	{ 0.0, 359.0 }
fetch (km)	{ 25.0, 200.0 }
patch size (m)	{ 400.0, 4000.0 }
patch dimensions (pixels)	2048 \times 2048
depth (km)	1000.0

Table 1: Simulation parameters for an ocean surface based on the TMA spectrum. A value for each parameter is chosen from a uniform distribution within the indicated range. Some parameters have only a single value and do not vary.

whitecap fraction via the MOM80 model [1]

$$W = 3.84 \times 10^{-6} U^{3.41} \quad (14)$$

which in turn produced a value for λ_T via the implicit equation 13 and $\alpha = 0.861$. The simulations were run for 300 frames, with a time step of $1/30sec$, and the whitecap fraction averaged over the last 100 frames. Figure 7 shows whitecap fractions from the ocean surface realizations, compared to the phenomenological curve for MOM80. As many authors of have noted while analyzing observational whitecap data, the mechanisms producing whitecap fraction are many and not all described by a dependence on wind speed alone [3]. Similarly, our model of whitecap generation and evolution is sensitive to many more influences that just wind speed, and so the whitecap fraction realizations should be distributed around the model curve. In both observational analysis studies and the model fitting here, the characterization of whitecap fraction in terms of windspeed is a useful organizational mechanism. In fact, the scatter of data points in figure 7 bears a superficial resemblance to the scatter of observational data (see, for example, figure 2 in [8]). Other whitecap fraction models that phenomenologically account for dependence on more oceanographic conditions may also provide opportunities for modeling of λ_T with more specific detail.

Figure 8 shows the whitecap opacity fields generated in three of the random realizations in figure 7, representing a broad range of whitecap conditions generated. One of these cases is in the rendered ocean scene displayed in figure 1. The whitecap opacity map $O(\mathbf{x}, t)$ is shaded as a white lambertian texture on the surface.

6 Conclusions

In many computer graphics applications, generating ocean whitecaps via the minimum eigenvalue threshold has been the method of choice, while the pa-

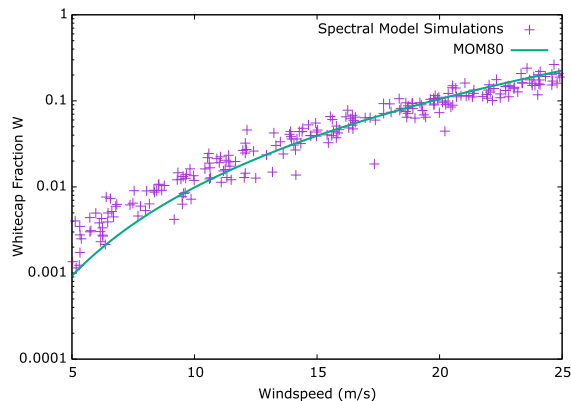


Figure 7: Whitecap fractions obtained from simulations, in which the threshold parameter λ_T is chosen via algorithm 1, with the value $\alpha = 0.861$, or $\Delta t = 0.15T$.

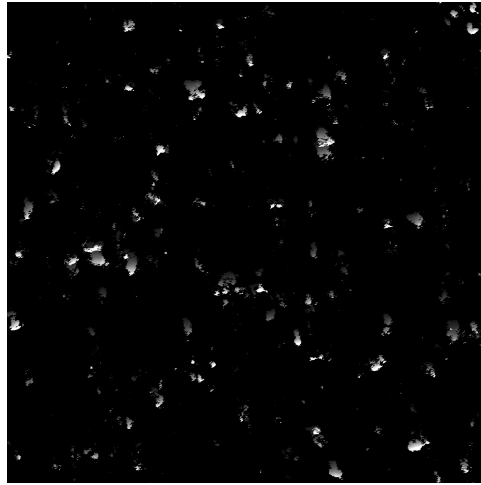
parameters involved have been user-chosen without much regard for ocean phenomenology. Here a method has been demonstrated for making those choices based on ocean phenomenology and the probability density function of the minimum eigenvalue. Because whitecap formation and decay depends on more than just windspeed, the simulated whitecap fraction randomly deviates from the phenomenological prediction. Overall however, this algorithm provides a phenomena-driven and realization-sensitive process for assigning the threshold parameter to achieve a physically-reasonable amount of whitecaps.

Acknowledgements

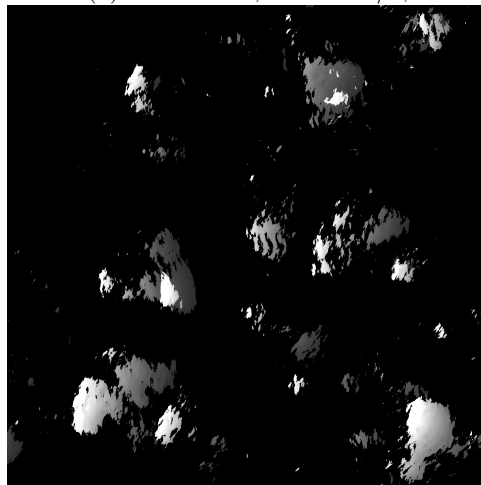
This work was supported in part under Navy Contract N6600118P0319.

References

- [1] M. F. M. A. Albert, M. D. Anguelova, A. M. M. Manders, M. Schaap, and G. de Leeuw. Parameterization of oceanic whitecap fraction based on satellite observations. *Atmospheric Chemistry and Physics*, 16(21):13725–13751, 2016.
- [2] H. Bowles. Crest: Novel Ocean Rendering Techniques in an Open Source Framework. In *SIGGRAPH 2017 - ACM SIGGRAPH Conference and Exhibition on Computer Graphics and Interaction Techniques*, Los Angeles, California, Aug. 2017. ACM.



(a) $W = 0.012$, $U = 12m/s$;



(b) $W = 0.044$, $U = 14m/s$



(c) $W = 0.15$, $U = 23m/s$

Figure 8: Examples of whitecap maps from several whitecap fractions.

- [3] S. E. Brumer, C. J. Zappa, I. M. Brooks, H. Tamura, S. M. Brown, B. W. Blomquist, C. W. Fairall, and A. Cifuentes-Lorenzen. Whitecap coverage dependence on wind and wave statistics as observed during so gasex and hiwings. *Journal of Physical Oceanography*, 47(9):2211–2235, 2017.
- [4] E. Darles, B. Crespin, D. Ghazanfarpour, and J. Gonzato. A survey of ocean simulation and rendering techniques in computer graphics. *CoRR*, abs/1109.6494, 2011.
- [5] J. Dupuy and E. Bruneton. Real-time Animation and Rendering of Ocean Whitecaps. In *SIGGRAPH Asia 2012 - 5th ACM SIGGRAPH Conference and Exhibition on Computer Graphics and Interaction Techniques in Asia*, SA '12 SIGGRAPH Asia 2012 Technical Briefs, page Article No. 15, Singapour, Singapore, Nov. 2012. ACM.
- [6] S. T. Grilli, J. Horrillo, and S. Guignard. Fully nonlinear potential flow simulations of wave shoaling over slopes: Spilling breaker model and integral wave properties. *Water Waves*, Oct 2019.
- [7] C. J. Horvath. Empirical directional wave spectra for computer graphics. In *Proceedings of the 2015 Symposium on Digital Production, DigiPro '15*, pages 29–39, New York, NY, USA, 2015. ACM.
- [8] C. Lafon, J. Piazzola, P. Forget, O. Le Calve, and S. Despiau. Analysis of the variations of the whitecap fraction as measured in a coastal zone. *Boundary-Layer Meteorology*, 111(2):339–360, May 2004.
- [9] D. M. Milder. The effects of truncation on surface-wave hamiltonians. *Journal of Fluid Mechanics*, 217:249–262, 1990.
- [10] D. J. Salisbury, M. D. Angelova, and I. M. Brooks. On the variability of whitecap fraction using satellite-based observations. *Journal of Geophysical Research: Oceans*, 118(11):6201–6222, 2013.
- [11] R. A. Smith. An operator expansion formalism for nonlinear surface waves over variable depth. *Journal of Fluid Mechanics*, 363:333–347, 1998.
- [12] F. Suriano. An introduction to realistic ocean rendering through fft, 2017.
- [13] J. Tessendorf. Simulating ocean water. *SIGGRAPH'99 Course Note*, 08 2001.
- [14] E. S. Tse, J. McGill, and R. L. Kelly. Coherent whitecap and glitter simulation model. In R. W. Spinrad, editor, *Ocean Optics X*, volume 1302, pages 505 – 519. International Society for Optics and Photonics, SPIE, 1990.
- [15] H. Wang, Y. Yang, C. Dong, T. Su, B. Sun, and B. Zou. Validation of an improved statistical theory for sea surface whitecap coverage using satellite remote sensing data. *Sensors*, 18(10), 2018.